Lead sorption by sea nodule residue generated in reduction roasting – ammonia leaching.

N. S. Randhawa* and R. K. Jana

CSIR-National Metallurgical Laboratory, Jamshedpur – 831007, Jharkhand, INDIA

*Corresponding author.
nsr@nmlindia.org

ABSTRACT: Residue generated in reduction roast – ammonia leaching of sea nodules has been utilised for the remediation of aqueous lead. Characterization of sea nodule residue (SNR) reveals fine granulometry (d_{50} = 11.4 µm) and high surface area of 66.7 m^2 g^{-1}. Batch adsorption experiments have been performed varying different parameters. Equilibrium experimental data fitted well in the Langmuir isotherm and derived maximum adsorption capacity (q_m) of lead onto SNR has been found to be 840.34 mg Pb(II)/g SNR at 303 K. The q_m enhanced to very high value of 2500 mgPb/gSNR upon raising the temperature to 323 K. The pseudo second-order model has been found applicable to the lead removal kinetics.

KEYWORDS: adsorption; leach residue; lead; sea nodule.

1. INTRODUCTION

Heavy metals containing effluent has been seen as threat to the environment due to its hazardous nature. Among various remediation techniques, removal of heavy metals from effluents by adsorption onto a low cost adsorbent, especially the waste category, has been investigated in the recent past. The residues/wastes generated in $NH_4OH/(NH_4)_2SO_4$ and $NH_4OH/(NH_4)_2CO_3$ leaching of sea nodules have been successfully employed in adsorptive remediation of several anionic (PO_4^{3-}, SeO_3^{2-}, $Cr_2O_7^{2-}$ etc.) and cationic (Cd^{2+}, Cu^{2+}, Ni^{2+} etc.) pollutants from waste waters (Parida et al. 2004a, 2004b; Agrawal et al. 2004, 2005; Das and Jana 2006; Mallick et al. 2006; Agrawal and Sahu 2006; Dash and Parida 2007; Randhawa et al. 2012, 2013). However, lead adsorption from waste water/effluents has not been studied in details with the leached residue generated in reduction roast-ammonia leaching process of sea nodules (Jana et al. 1999). The aqueous lead pollution originates from industrial activities such as mining, smelting operations, battery manufacture and recycling etc, which generate

huge amount of lead containing effluents and waste water. Contamination of lead in drinking water, even in low concentration, may cause diseases such as anemia, hepatitis, nephrine syndrome etc (Barbosa et al. 2005). Lead has also been found to be responsible for neurotoxicity of central and peripheral nervous systems (Hsiang and Diaz 2012). In view of this, present study has been aimed at investigating the sorption properties of residue, generated in the $NH_4OH/(NH_4)_2CO_3$ leaching of sea nodules, for the removal of lead from its aqueous solution. To carry out the investigation, several parameters have been varied to determine lead adsorption characteristics of sea nodules leach residue.

2. EXPERIMENTAL

2.1 Material

The sea nodule residue (SNR) has been obtained from large scale reduction roasting - ammoniacal leaching trial of sea nodules. For characterization and sorption studies, SNR is washed with deionised water to remove the entrapped leach liquor followed by air-drying for several days.

2.2 Characterization of SNR

For chemical analyses, a weighed quantity of SNR is digested in acid (HCl/HNO_3 mixture), dehydrated, redissolved in HCl (1:1) and filtered. The dehydrated silica is estimated gravimetrically while major and minor constituents in the filtrate are analysed by conventional wet chemical methods (Vogel 1978) and Atomic Absorption Spectrometer (Perkin Elmer AAnalyst 400), respectively. Surface area measurement and pore size analysis are conducted using Quantachrome 4000E surface area analyser (Nova Instruments, USA). Size analysis of SNR is carried out in Malvern Mastersizer after ultrasonic liberation of particles. Point of zero charge of SNR is determined acid-base titration method reported by Huang and Ostavic (1978). The microscopic features of the samples are characterized by scanning electron microscope (FEI Nova NanoSEM 430).

2.3 Lead removal studies

The synthetic stock solution of lead (Pb(II)) of 1000 mg L^{-1} is prepared by dissolving 1.598 g $Pb(NO_3)_2$ in deionised water. Solutions of 0.01M HNO_3 and 0.01M NaOH are used for pH adjustment with the help of digital pH meter (Toshniwal CL46) after calibration with

National Bureau of Standards buffers. 0.1N KNO_3 is used to maintain the ionic strength in all the adsorption experiments. All the chemicals are AR grade and procured from Merck Specialities Pvt. Ltd., Mumbai. ASTM grade I deionised water is used in all the experimental and analytical investigations. Pb(II) removal characteristics of SNR are evaluated by batch kinetics and equilibrium experiments. For kinetic studies, typically, 100 mL of Pb(II) solution at desired concentration with appropriate amounts of SNR is taken in a 250 mL stoppered conical flask. After adjusting to required pH and flask is shaken using a water bath shaker, maintained at desired temperature. Samples are withdrawn at certain time interval and the SNR is separated by filtration/centrifugation. The remaining Pb(II) in the filtrate is analyzed by atomic absorption spectrometer (PerkinElmer AAanalyst400). The amount of Pb(II) adsorbed per gram of the SNR, Q_t (mg g^{-1}) at time t is calculated using Eq. (1).

$$Q_t = \frac{(C_o - C_t)\,V}{w \times 1000} \tag{1}$$

Where, C_o and C_t are the initial Pb(II) concentration (mg L^{-1}) and Pb(II) in solution respectively, and V is the volume of solution in mL and w the mass of sorbent in gram. The equilibrium adsorption experiments are carried out to investigate the effect of various parameters, such as pH (3-9) of the Pb(II) solution, initial Pb(II) concentration (50-1000 mg L^{-1}), SNR dose (25-2000 mg L^{-1}) and temperature (303-323 K) under fixed equilibration time obtained by preliminary kinetic experiments.

3. RESULTS AND DISCUSSION

3.1 Characterization of SNR

Detailed chemical analysis of sea nodule residue (SNR) is given in Table 1. The manganese, iron and silicon are the major constituents along with lime, magnesia and alumina. Fig. 1 shows the SEM image of SNR, which reveals aggregated bodies of small particles of various sizes. The particle size determination indicates fine nature of SNR with mean particle diameter (d_{50}) of 11.4 µm. Surface area is determined as 66.7 m^2 g^{-1} in SNR. The pH$_{pzc}$ of SNR, determined by titremetric procedure, is found to be about 6.5, which is higher than that reported for sea nodules (4.5-4.7) (Bhattacharjee et al. 2003; Parida et al. 1996). Detailed XRD and FT-IR characterisation of SNR have been carried out previously which showed presence of $MnCO_3$, Mn_2SiO_4 and $Mn_2SiO_3(OH)_2 \cdot H_2O$ phases (Behera et al. 2010; Randhawa et al. 2013). Absorption bands in FT-IR spectrum of SNR at 1470 cm^{-1},

3

1070 cm^{-1} and 870 cm^{-1} are attributed to the ν(C–O) and δ(OCO) vibrations of the carbonate ion (Behera et al. 2010). Both XRD and FT-IR characterisation of SNR confirms the presence of MnCO$_3$ in SNR which may have formed during the reduction–roasting–ammonia leaching of sea nodules.

Table 1 Chemical composition of SNR.

| Element/radical	Wt.-%
Mn	26.11
Fe	10.19
SiO$_2$	16.44
Al$_2$O$_3$	3.54
CaO	0.36
MgO	4.40
Co	0.039
Ni	0.05
Cu	0.13
Moisture	6.18
LOI	17.01
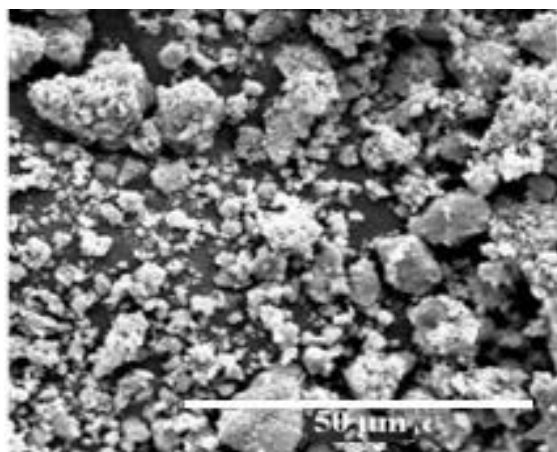
Fig.1 Secondary electron image of SNR

3.2 Pb(II) sorption studies

3.2.1 Effect of time and initial Pb(II) content

4

The effect of time on Pb(II) removal by SNR, studied with the solutions containing 50, 100, 150, 200, 500 and 1000 mg L^{-1} Pb(II), SNR dose of 100 mg L^{-1}, pH 5.5 at 303 K, is depicted in Fig. 2. Both the contact time between SNR and Pb(II) and initial concentration of Pb(II) have significant influence on the adsorption of Pb(II) onto SNR. Two types of adsorption patterns are apparent: initial fast adsorption and then slowly reaching equilibrium in all the cases.
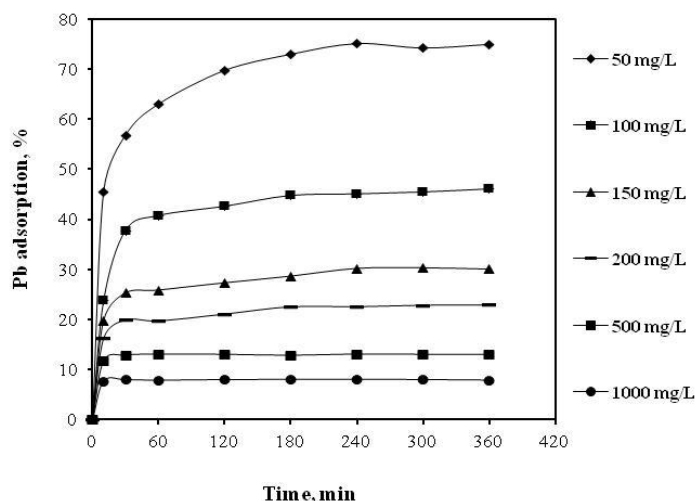

Fig. 2 Effect of time and initial Pb(II) concentration on lead removal with SNR dose of 100 mg L^{-1}, pH 5.5 at 303 K.

In the case of initial Pb(II) concentrations <500 mg L^{-1}, fast adsorption takes place in the initial 10 min adsorbing more than 50% of the total adsorption value, then reaching slowly to the equilibrium in about 240 min. On the other hand, equilibrium is attained rapidly (within 30 min) in case of initial Pb(II) ≥500 mg L^{-1}. The faster adsorption of Pb(II) under identical conditions (pH ~ 5.5) for initial Pb(II) ≥500 mg L^{-1} may be due to better interaction between the adsorbent surface and abundant Pb(II) ions at high initial concentration. The initial Pb(II) concentration also affects amount of adsorption on SNR. Highest adsorption percent of Pb(II) is obtained at the lowest concentration of Pb(II) i.e. 50 mg L^{-1} and adsorption decreases with increasing initial Pb(II) concentration.

3.2.2 Effect of pH

The effect of pH on the adsorption of Pb(II) is studied by varying the initial pH of solution from 3 to 9, which is presented in Fig. 3. It is observed that the adsorption of Pb(II) increases with the pH of solution. The increase in lead adsorption can be partly attributed to

formation of different hydroxo species with rise of solution pH. The species distribution diagram for Pb(II) shows that Pb^{2+} is predominant (>95%) species up to pH 6 whereas hydroxo and dihydroxo species are formed after pH 7 (Das and Jana 2006). Thus, removal of Pb(II) up to pH 6 is due to adsorption of Pb^{2+} over SNR surface whereas at pH > 6 precipitation of hydroxo anion i.e. $Pb(OH)^+$ as hydroxide over SNR surface plays dominant role in the removal of Pb(II). Another reason may be the abundance of hydronium (H_3O^+) ions in the solution (Das and Jana, 2006; Agrawal and Sahu, 2006). At low pH values, the solution has an excess of H_3O^+ ions and hence a competition exists between the positively charged H_3O^+ ions and Pb(II) ions for the available negative adsorption sites on the SNR surface. As the pH increases and the concentration of H_3O^+ lowers, more of the positively charged metal ions in solution are adsorbed on the SNR.
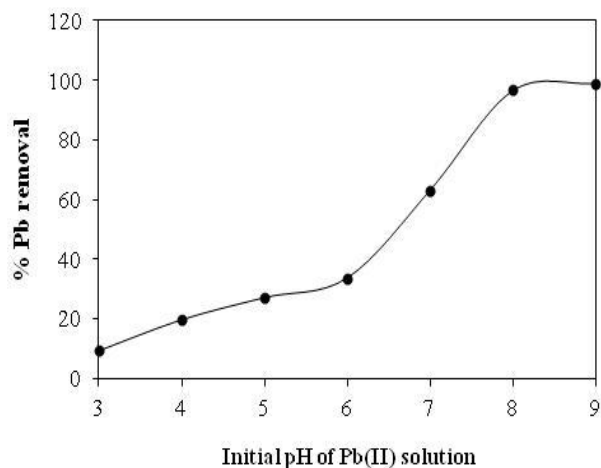
Fig. 3 Effect of solution pH on Pb(II) removal with SNR dose of 100 mg L^{-1}, initial Pb(II) 100 mg L^{-1} at 303 K and shaking time 240 min.

3.2.3 Effect of SNR dose

To study the effect of SNR dose on Pb(II) removal characteristics, different amounts of SNR (50-1000 mg L^{-1}) are shaken with 100 ml of Pb(II) solution (100 mg L^{-1}) for 240 min at pH 5.5. It is observed that the equilibrium Pb(II) concentration (C_e) decreases with increasing SNR addition, as shown in Fig. 4. The positive correlation between adsorbent dose and Pb(II) removal efficiency can be related to the increasing available surface area or binding sites. Nearly 100% Pb(II) removal is achieved with 1000 mg L^{-1} SNR dose.

6
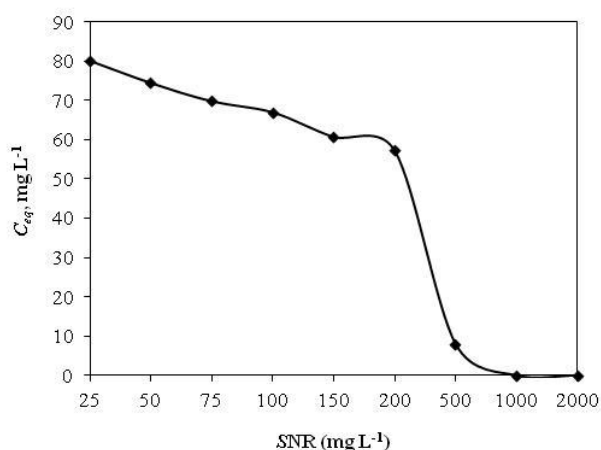
Fig. 4 Effect of SNR dose on Pb(II) removal with initial Pb(II) 100 mg L^{-1}, pH 5.5 at 303 K and shaking time 240 min. Variations in Pb(II) remaining in the solution at equilibrium (C_e) after shaking with certain dose of SNR are shown.

3.2.4 Pb(II) removal kinetics

The kinetic studies of Pb(II) sorption on SNR are carried out with 100 mg L^{-1} Pb(II) solution at pH 5.5 and SNR dose of 100 mg L^{-1} at temperatures of 303, 313 and 323 K. Data from these experiments is fitted into pseudo first-order model (Eq. 3) and pseudo second-order model (Eq. 4) to estimate the specific rate constants (Ho 2004; Ho 2006).

$$\ln(q_e - q_t) = \ln q_e - k_1 t \tag{3}$$

$$\frac{t}{q_t} = \frac{1}{k_2 q_e^2} + \frac{1}{q_e t} \tag{4}$$

Where, q_e and q_t refer to the amount of Pb(II) adsorbed per unit weight of adsorbent (mg g^{-1}) at equilibrium and at any time t (min). k_1 and k_2 are the pseudo first-order and pseudo second-order rate constants, respectively. The term $k_2 q_e^2$ in Eq. (4) denotes the initial sorption rate ($h_{0,}$ mg g^{-1} min^{-1}).

$$h_0 = k_2 q_e^2 , \tag{5}$$

The plot of $\ln(q_e - q_t)$ versus t and t/q_t versus $1/q_e$ are plotted to calculate the rate constants yielding straight lines. The calculated parameters of kinetic models (Table 2) show that adsorption of Pb(II) on SNR obeys pseudo second-order rate kinetics (higher values of r^2) more than the pseudo first-order rate kinetics. The Pb(II) removal at equilibrium (q_e)

7

change significantly when temperature increases from 303 K to 323 K. This indicate chemical interaction/bonding during Pb(II) adsorption onto SNR, since decrease in sorption capacity with increase in temperature has been found responsible for adsorption by physical phenomena (Srivastava et al. 2006).

Table 2 Pseudo first-order and pseudo second-order rate constants for adsorption of Pb(II) onto SNR at temperatures 303-313-323 K.

Temp, K	Pseudo first-order model			Pseudo second-order model			
	k_1 min^{-1}	q_e cal. mg g^{-1}	r_1^2	k_2 g mg^{-1} min^{-1}	q_e cal. mg g^{-1}	h_o mg g^{-1} min^{-1}	r_2^2
303	0.010	320.95	0.792	0.00013	476.19	29.15	0.996
313	0.012	316.87	0.919	0.00015	588.24	51.28	0.999
323	0.012	341.17	0.748	0.00017	625.00	67.11	0.998

3.2.5 Isotherm studies

To characterize the equilibrium between the amount of adsorbate that accumulate on the adsorbent and the concentration of the dissolved adsorbate, the equilibrium Pb(II) adsorption data are fitted by both the Langmuir (Eq. 6) and the Freundlich (Eq. 7) models (Das and Jana, 2006; Dash and Parida, 2007). The coefficients of these models are computed using linear least-squares fitting.

$$\frac{C_e}{q_e} = \frac{1}{bq_m} + \frac{C_e}{q_m}$$

(6)

$$\ln q_e = (1/n) \ln C_e + \ln K_f$$

(7)

Where q_e is the equilibrium adsorption capacity, mg g^{-1}; C_e is equilibrium liquid phase concentration, mg L^{-1}; q_m is the maximum adsorption capacity, mg g^{-1} and b is adsorption equilibrium constant, L g^{-1}. The K_f and $1/n$ stand for empirical constants related to adsorption capacity and intensity, respectively for Freundlich model. The value of b and q_m are calculated from the intercept and slope of the plot between C_e / q_e and C_e whereas K_f and $1/n$ are calculated from intercept and slope of the plot between $\ln q_e$ and $\ln C_e$. The calculated

8

parameters from Langmuir and Freundlich isotherm plots at 303, 313 and 323 K are given in Table 3.

Table 3 Calculated Langmuir and Frundlich isotherms parameters.

Temp, K	Langmuir isotherm			Freundlich isotherm		
	Adsorption maxima	Binding energy constant	Regression coefficient	Adsorption capacity	Adsorption intensity	Regression coefficient
	q_m (mg g^{-1})	b (mg L^{-1})$^{-1}$	r^2	K_f (mg g^{-1})	$1/n$	r^2
303	840.34	0.033874	0.999	264.42	0.173	0.924
313	1351.35	0.01808	0.999	494.31	0.141	0.987
323	2500.00	0.015026	0.999	726.11	0.158	0.981

On the basis of regression coefficient, the isotherm data fits better with the Langmuir model than the Freundlich model. The increase in the value of q_m with the increasing temperature confirms endothermic nature of Pb(II) – SNR interaction in aqueous solution. The maximum adsorption capacity (q_m) derived from Langmuir isotherm is 840.34 mg Pb(II)/g SNR at 303 K. Raising the temperature to 313 K enhanced the Pb(II) uptake by SNR to 1351.35 mg Pb(II)/g SNR and further to 2500 mg Pb(II)/g SNR at 323 K, which is considerably higher than the so far reported highest Pb(II) adsorbing material i.e. Nano-MgO, q_m = 1980 mg g^{-1} (Cao et al. 2012). Thus, very high loading capacity coupled with fast kinetics make SNR a potential material for remediation of Pb(II) contaminated effluents.

4. CONCLUSION

The sea nodules residue (SNR) has been characterized and investigated for adsorptive removal of Pb(II) from aqueous solution. Characterization studies have showed that SNR is ~~was~~ amorphous in nature with high surface area (66.7 m^2 g^{-1}). The SEM studies have revealed random aggregates of SNR particles. The SNR has been found to be highly efficient adsorbent for Pb(II) in aqueous solution. The adsorption equilibrium is seen dependent on initial concentration of Pb(II) ion: ~4 h for <500 Pb(II) mg L^{-1} and 30 min for ≥500 mg L^{-1}. Based on regression analysis, pseudo-second order kinetic has been found to be applicable for the Pb(II) adsorption indicating chemisorption. The Pb(II) uptake data has shown good fit

to Langmuir isotherm than the Freundlich isotherm. The maximum removal capacity of Pb(II) by SNR, determined by Langmuir model, is 840.34 mg g^{-1} at 303 K, which improves to 2500 mg g^{-1} at 323 K. This study has demonstrated an efficient application of sea nodule residue to solve the environment problems associated with the highly health hazardous lead contaminated industrial effluents as well as the utilization of sea nodules processing residues/wastes.

ACKNOWLEDGMENT

REFERENCES

Acharya, R., Ghosh, M.K., Anand, S., Das, R.P. 1999. Leaching of metals from Indian Ocean nodules in SO_2–H_2O–H_2SO_4–$(NH_4)_2SO_4$ medium. Hydrometallurgy. 53, 169-175.

Agrawal, A., Sahu, K.K., 2006. Kinetic and isotherm studies of cadmium adsorption on manganese nodule residue. J. Hazard. Mater. B137, 915–924.

Agrawal, A., Sahu, K.K., Pandey, B.D., 2004. A comparative adsorption study of copper on various industrial solid wastes. AIChE J. 50, 2430-2438.

Agrawal, A., Sahu, K.K., Pandey, B.D., 2005. Systematic studies on adsorption of lead on sea nodule residues. J. Colloid Interf. Sci. 281, 291–298.

Barbosa Jr., F., Tanus-Santos, J.E., Gerlach, R.F., Parsons, P.J., 2005. A critical review of biomarkers used for monitoring human exposure to lead: advantages, limitations, and future needs. Environ. Health Perspect. 113, 1669-1674.

Behera, R.K., Satapathy, P.K., Randhawa, N.S., Das, N.N., 2010. Adsorptive removal of phosphate ions using leached sea nodule residue generated by the reduction–roasting ammoniacal leaching process. Adsor. Sci. Technol. 28, 611-627.

Bhattacharjee, S., Chakrabarty, S., Maity, S., Kar, S., Thakur, P., Bhattacharyya, G., 2003. Removal of lead from contaminated water bodies using sea nodule as an adsorbent. Water Res. 37, 3954-3966.

Cao, C.Y., Qu, J., Wei, F., Liu, H., Song, W.G., 2012. Superb adsorption capacity and mechanism of flowerlike manganesium oxide nanostructures for lead and cadmium ions. ACS Appl. Mater. Interfaces. 4, 4243-4287.

Das, N.N., Jana, R.K., 2006. Adsorption of some bivalent heavy metal ions from aqueous solutions by manganese nodule leached residues. J. Colloid Interf. Sci. 293, 253–262.

Dash, S.S., Parida, K.M., 2007. Studies on selenite adsorption using manganese nodule leached residues. J. Colloid Interf. Sci. 307, 333–339.

Ho, Y.S., 2004. Citation review of Lagergren kinetic rate equation on adsorption reactions. Scientometrics. 59, 171–177.

Ho, Y.S., 2006. Review of second-order models for adsorption systems, J. Hazard. Mater. 136, 681–689.

Hsiang, J., Díaz, E.., 2011. Lead and developmental neurotoxicity of the central nervous system. Current Neurobiol. 2, 35-42.

Huang, C.P., Ostavic, F.G., 1978. Removal of Cd(II) by activated carbon adsorption. J. Environ. Eng. Div. 104, 863–878.

Jana, R.K., Srikanth, S., Pandey, B.D., Kumar, V., Premchand, 1999. Processing of deep sea manganese nodule at NML for recovery of copper, nickel and cobalt. Met. Mater. Proc. 11, 133-139.

Mallick, S., Dash, S.S., Parida, K.M., 2006. Adsorption of hexavalent chromium on manganese nodule leached residue obtained from NH_3–SO_2 leaching. J. Colloid Interf. Sci. 297, 419–425.

Parida, K.M., Satapathy, P.K., Das, N., 1996. Studies on Indian Ocean Manganese Nodules: IV. Adsorption of some bivalent heavy metal ions onto ferromanganese nodules. J. Colloid Interf. Sci. 181, 456-462.

Parida, K.M., Mallick, S., Dash, S.S., 2004a. Studies on manganese nodule leached residues 2. Adsorption of aqueous phosphate on manganese nodule leached residues. J. Colloid Interf. Sci. 290, 22–27.

Parida, K.M., Mallick, S., Mohapatra, B.K., Misra, V.N., 2004b. Studies on manganese-nodule leached residues 1. Physicochemical characterization and its adsorption behavior toward Ni^{2+} in aqueous system. J. Colloid Interf. Sci. 277, 48–54.

Randhawa, N.S., Das, N.N., Jana, R. K., 2012. Selenite adsorption using leached residues generated by reduction roasting–ammonia leaching of manganese nodules. J. Hazard. Mater. 241–242, 486– 492.

Randhawa, N.S., Das, N.N., Jana, R.K., 2013. Adsorptive remediation of Cu(II) and Cd(II) contaminated water using manganese nodule leaching residue. Desal. Water Treat. (In press) DOI:10.1080/19443994.2013.801324.

Srivastava, V.C., Mall, I.D., Mishra, I.M., 2006. Characterization of mesoporous rice husk ash (RHA) and adsorption kinetics of metal ions from aqueous solution onto RHA. J. Hazard. Mater. 134, 257-267.

Vogel, A.I., 1978. A text book of quantitative inorganic analysis. 4th Edn. Longmans, London.